Two-Dimensional Electrical Properties Tomography Using a Simplified Contrast-Source Inversion Approach

Patrick Fuchs
Circuits and Systems, Microelectronics Department
Delft University of Technology
Delft, The Netherlands
p.s.fuchs@tudelft.nl

Rob Remis
Circuits and Systems, Microelectronics Department
Delft University of Technology
Delft, The Netherlands
r.f.remis@tudelft.nl

***Abstract*—The contrast source inversion (CSI) method is a well-known inversion technique that has been utilized in a wide range of application areas. Here we show that in the specific situation of electrical properties tomography (EPT) in magnetic resonance imaging (MRI), which is a so-called hybrid inverse problem, since data is collected inside the reconstruction domain, the CSI method can be simplified to what is essentially a single forward simulation provided the electromagnetic field has an E-polarized field structure. As a consequence, the computational costs are significantly reduced and our experiments show that reconstructions obtained with the simplified CSI method have essentially the same accuracy as reconstructions obtained with the full CSI inversion method.**

***Index Terms*—Electrical Tissue Properties, Electromagnetic Inversion, Magnetic Resonance Imaging, Optimization.**

I. Introduction

Magnetic resonance imaging (MRI) is a powerful imaging modality that can be used not only for imaging tissue contrasts but also to image the *in vivo* electrical properties of different tissue types. Specifically, in electrical properties tomography (EPT) the objective is to retrieve the conductivity and permittivity tissue profiles at the MR frequency of operation (Larmor frequency) and within an inversion domain of interest based on measured magnetic flux density data (the B_1^+-field) that has its support *inside* the inversion domain.

It has been shown in [1] that the contrast-source inversion (CSI) method applied to EPT (CSI-EPT) is able to retrieve the conductivity and permittivity maps within a domain of interest even for strongly inhomogeneous tissue profiles. However, convergence may be slow and it may take the CSI-EPT method many iterations to reach the desired error tolerance.

Fortunately, computation times and costs can be significantly reduced by taking advantage of the field structure that may be present inside the imaging domain of interest and the fact that data collection takes place inside this imaging domain. Specifically, we show that for two-dimensional field structures which can occur in the midplane of a birdcage coil [2], it is possible to image the induced currents in real-time and the electrical tissue maps in this plane can be obtained within at most a couple of seconds on a standard laptop or PC by solving a single forward problem. Since the simplified CSI-EPT method does rely on an E-polarized field structure, it is more limited in its applicability than standard CSI-EPT, but if it can be applied then significant speedups can be realized and accurate tissue profiles may be obtained at reduced computational costs.

In previous work this has been shown for a head model, but to show that the method can handle larger domains where the speedup is even more significant here we focus on the computationally more challenging abdomen.

II. Method

In the midplane of a birdcage coil, the electromagnetic field is essentially E-polarized meaning that the electric field strength has a longitudinal z-component only, while the magnetic field is purely transverse (see [2] for a detailed discussion). With σ and ε denoting the conductivity and permittivity within the midplane of the coil, the induced electric-current density in this plane is given by:

$$J_z^{\text{ind}} = (\sigma + \mathrm{j}\omega\varepsilon)E_z. \tag{1}$$

The electric field strength E_z and the medium parameters σ and ε are all unknown, of course. Now in MRI, the so-called B_1^+ field:

$$B_1^+ = \frac{B_x + \mathrm{j}B_y}{2}, \tag{2}$$

can be measured inside the object in the midplane of a birdcage coil. Given a B_1^+ measurement, and introducing the differentiation operator $\partial^- = (\partial_x - \mathrm{j}\partial_y)/2$, it follows from Ampere's law and the fact that the magnetic flux density is divergence free that:

$$J_z^{\text{ind}} = \frac{4}{\mathrm{j}\mu_0}\partial^- B_1^+. \tag{3}$$

In other words, the induced current follows from a first-order spatial differentiation of the B_1^+-data and the present method is therefore called foIC-EPT (first-order induced-current EPT). In practice, the data is typically filtered to avoid

978-0-9960078-8-7©2019 ACES

noise amplification. Clearly, computing the induced current density can be realized essentially in real-time.

Having the induced current available, the electric field strength within the midplane can be obtained by solving a particular integral equation for the electric field strength presented in [3]. Solving this equation is equivalent to solving a forward problem and its solution can be obtained efficiently using iterative solvers such as CG-FFT or GMRES.

Finally, the conductivity and permittivity can be determined using the constitutive relation of equation (1), since the induced current density J_z^{ind} and the electric field strength E_z are now known. Note that at locations where the magnitude of the electric field strength is small it is difficult to retrieve the tissue parameters from the constitutive relation of equation (1).

III. Results

Simulations are performed to compare midplane tissue profile reconstructions obtained with CSI-EPT and the reconstruction method outlined above. Ideal B_1^+ data was obtained by simulating the wave field response due to 16 equally spaced line sources positioned on a circle with a radius of 34 cm that operate in quadrature mode at 128 MHz, which is the operating frequency that corresponds to a 3 tesla background field. For noiseless data, foIC-EPT and CSI-EPT produce essentially identical reconstructions. Therefore, to provide a more accurate representation of actual measured data, we corrupted the simulated B_1^+ data with noise at an SNR of 40dB. The current simplified reconstruction method and CSI-EPT were both implemented in Matlab 2018b on a desktop computer with an Intel i5 processor and 8Gb of RAM. Further implementation details can be found in [3].

Figures 1 (a) and 1 (d) show the exact conductivity and permittivity maps of a thorax model positioned at the midplane of the birdcage coil. Figures 1 (b) and 1 (c) show the conductivity reconstructions obtained with foIC-EPT and CSI-EPT, respectively. The corresponding permittivity reconstructions are shown in Figs 1 (e) and 1 (f). The normalised global error for the conductivity and permittivity are 0.118 and 0.1399 for foIC-EPT and 0.1157 and 0.1342 for CSI-EPT methods respectively. The CSI-EPT reconstruction took 278 iterations (49.5 seconds) for the normalized residual to drop below the noise level, while five GMRES iterations were required to solve the E-field integral equation (normalized residual smaller than 10^{-6}) and it took 0.21 seconds for foIC-EPT to obtain the tissue reconstructions presented in Figs 1 (b) and 1 (e).

IV. Discussion and Conclusion

In quadrature mode, the magnitude of the electric field strength is relatively small in an area around the center of the slice, and for both methods the effects of noise are clearly seen in this area. For foIC-EPT these noise effects are stronger due to the differentiation of the data (equation (3)). Such a step is absent in the CSI-EPT method. Noise effects can be suppressed, of course, by incorporating regularization techniques in both reconstruction methods. In addition, at 3T (128 MHz) both methods produce lower quality permittivity than the conductivity reconstructions since the conduction current dominates the induced current density at 128 MHz.

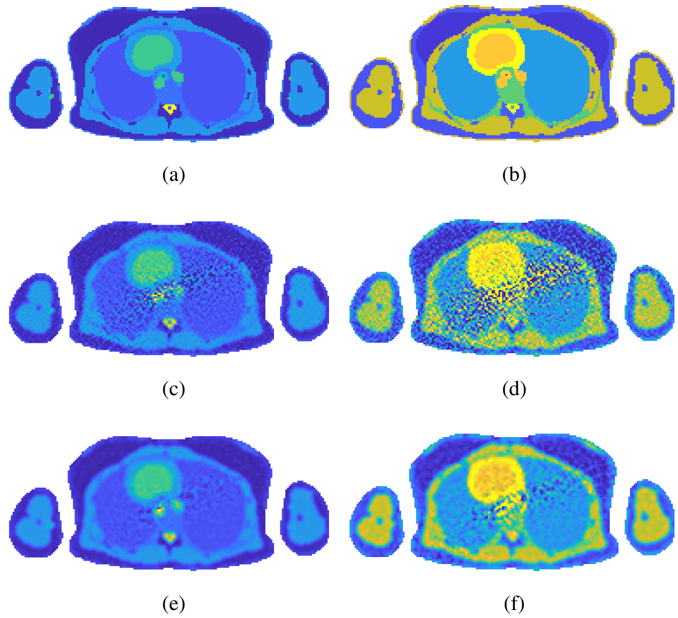

Fig. 1. (a), (c), (e), Conductivity profiles of a thorax slice; (a) is the original conductivity, (c) the foIC-EPT reconstruction, and (e) the 2D-CSI-EPT reconstruction. (b), (d), (f), permittivity profiles of a thorax slice; (b) is the original conductivity, (d) the foIC-EPT reconstruction, and (f) the 2D-CSI-EPT reconstruction.

In terms of computation time, the foIC-EPT method is 100 times faster for the region considered here, which allows for real-time imaging. The main computational cost of foIC-EPT and CSI-EPT is the computation of FFT-based matrix-vector products at every iteration, therefore, both have an equal complexity of $\mathcal{O}(n \log(n))$. For CSI-EPT, however, the total number of matrix-vector products that need to be computed is typically for thousands of iterations and foIC-EPT takes less than ten. We conclude that if the radiofrequency transmit field has a two-dimensional E-polarized field structure in some imaging plane of interest, then foIC-EPT is able to reconstruct these dielectric tissue profiles essentially in real time.

Acknowledgment

The authors would like to thank Reijer Leijsen from the Gorter Center for High-Field MRI, Leiden University Medical Center in The Netherlands for fruitful discussions.

References

[1] E. Balidemaj, et al., “CSI-EPT: A contrast source inversion approach for improved MRI-based electrical properties tomography,” IEEE Trans. Med. Imag., vol. 34, pp. 1788–1796, 2015.

[2] B. van den Bergen, C. C. Stolk, J. B. van den Berg, J. J. W. Lagendijk, and C. A. T. van den Berg, “Ultra fast electromagnetic field computations for RF multi-transmit techniques in high field MRI,” Phys. Med. Biol., vol. 54, pp. 1253–1264, 2009.

[3] P.S. Fuchs, et al., “First-order induced current density imaging and electrical properties tomography in MRI,” IEEE Trans. Comp. Imag., vol. 4, pp. 624–631, 2018.